

Production studies of D and B mesons at CMS

Valentina Mariani, on behalf of the CMS Collaboration^a

^a*Grant: 'L'Oréal Italia Per le Donne e la Scienza',
Association: INFN, Via A.Pascoli 23c, Perugia, Italy*

E-mail: vmariani@cern.ch

The large amount of data accumulated by the CMS experiment during the Run 2 of LHC offers robust probes for testing the Standard Model and potentially reaching beyond it. In this report the new CMS measurements of prompt D^{*+} , D^+ and D^0 production cross sections at 13 TeV are presented, together with novel studies of the production of excited B_c states carried out with full Run 2 data.

*40th International Conference on High Energy physics - ICHEP2020
July 28 - August 6, 2020
Prague, Czech Republic (virtual meeting)*

Introduction

Measurements of the production cross sections of beauty and charm mesons in hadronic collisions at high center-of-mass energies provide important tests of the theory of strong interactions known as quantum chromodynamics (QCD). Due in part to the presence of several competing scales (charm mass, transverse momentum) close to the threshold for the validity of the perturbative expansion, the related theoretical uncertainties are rather large. Furthermore, since the current calculations suffer from such large theoretical uncertainties, experimental constraints on heavy quark production cross sections are relevant for all the physics phenomena for which heavy quark production is an important background process. The Large Hadron Collider (LHC) is a powerful laboratory to study heavy flavour production, providing a wide kinematic range with a very high production cross section, if compared for example to the e^+e^- colliders. In these proceedings, the recent results on D and B meson production, obtained with the Compact Muon Solenoid (CMS) experiment will be presented.

1. Prompt open charm cross section measurement

The analysis presented here is a study on the charm meson production in pp collisions at $\sqrt{s} = 13$ TeV [1], focused on the measurement of cross sections for the prompt production of D^{*+} , D^0 , and D^+ mesons. The charm mesons are identified through the exclusive decays (where charge conjugation is implied): $pp \rightarrow D^{*+}X \rightarrow D^0\pi_{slow}^+X \rightarrow K^-\pi^+\pi_{slow}^+X$, $pp \rightarrow D^0X \rightarrow K^-\pi^+X$, and $pp \rightarrow D^+X \rightarrow K^-\pi^+\pi^+X$.

Data collected by CMS in 2016 have been analysed in a wide phase space, transverse momentum (p_T) between 4 and 100 GeV and the absolute value of the pseudorapidity ($|\eta|$) within 2.1. Since the very soft kinematic properties of the charm mesons, the most inclusive trigger, requiring only that a proton-proton collision occurred, is applied to select events. It is a heavily prescaled trigger, resulting in an integrated luminosity of 29 nb^{-1} , out of the 36.8 fb^{-1} collected in the 2016 data-taking period.

The single differential cross section for the charm mesons as a function of p_T is measured for the first time in pp collisions by the CMS Collaboration.

The signal is defined as prompt produced mesons, thus either produced directly from the pp interaction in the primary vertex (PV) or decaying from an excited charm mesons (as the D^0 coming from the D^* decay). The general reconstruction strategy for the three mesons is very similar. Charm mesons are reconstructed by combining two (three) tracks with the total charge 0 (1) for the D^0 (D^+) candidates, having an invariant mass M_{cand} within a specific range around the nominal mass of the mesons M^{PDG} [2]. In the p_T range relevant for the analysis, charged pions and kaons cannot be efficiently separated in the CMS detector. A kaon or pion mass hypothesis is thus assumed for the tracks, according to the charge and the specific decay channel. The two- or three-track combinations must be compatible with having a common secondary vertex (SV) with a vertex fit χ^2 probability greater than 1%. The cosine of the angle between the charm candidate momentum and the vector pointing from the PV to the SV must be greater than 0.99, thus requiring the D^0 or D^+ meson to be consistent with originating from the PV. This requirement greatly reduces the contribution from b hadron decays.

A requirement, specific to each meson, on the SV significance, defined as the distance between the PV and SV divided by its uncertainty, is also set. This is a crucial requirement in the analysis, since it refers to the specific topology of the decays and provides a considerable reduction in the combinatorial background. To complete the D^{*+} meson reconstruction, a third track with a looser selection, corresponding to the slow pion, is kinematically combined to the D^0 candidate.

The largest contribution to the background comes from random combinatorial candidates. The selection criteria, optimised for each of the reconstructed charm mesons, greatly reduce this contribution in favour of the signal events.

The charm meson differential cross section $d\sigma/dp_T$ is measured in 9 bins of p_T between 4 and 100 GeV in the range $|\eta| < 2.1$. The signal yields are determined using an unbinned maximum-likelihood fits to the invariant mass distributions for the various decay modes (the ΔM distribution, defined as $\Delta M = m(K\pi\pi_{slow}) - m(K\pi)$ is used for the D^{*+}) in each p_T bin. The signal components are modelled by the sum of two Gaussian functions with the same mean, to account for the nonuniform resolution over the detector acceptance, while the combinatorial background is described with different functions, according to the decay mode.

The nonprompt contribution, such as charm mesons coming from the b hadron decays, has been quantified using a simulated event sample. The contamination rate resulted to be between 5 and 17 % in the different p_T bins and it has been subtracted to the total visible cross section measured on data.

Several systematic uncertainties have been considered in the analysis. The dominant ones are the systematic related to the tracking efficiency 9.4, 4.2, and 6.1 % for the D^{*+} , D^0 , and D^+ mesons respectively, and the uncertainty on the signal and modelling that accounts for 3.8, 6.9, and 9 % for the D^{*+} , D^0 , and D^+ mesons.

The differential production cross sections, as a function of p_T , is defined as:

$$\frac{d\sigma(pp \rightarrow DX)}{dp_T} = \frac{N_i(D \rightarrow f)}{\Delta p_{Ti} BR(D \rightarrow f) \mathcal{L} \epsilon_{i,tot}(D \rightarrow f)} \quad (1)$$

where $N_i(D \rightarrow f)$ is the number of prompt charm mesons reconstructed in the selected final state for each bin i , Δp_T is the bin width, $BR(D \rightarrow f)$ is the branching fraction of the reconstructed final state, $\epsilon_{i,tot}(D \rightarrow f)$ is the total reconstruction efficiency of the decay chain evaluated using simulated events, and \mathcal{L} is the integrated luminosity.

Results of the $d\sigma/dp_T$ are reported in Fig 1 for the three mesons. Data (black points) are compared to different Monte Carlo (MC) models and theoretical predictions (horizontal lines and bands). The vertical error bars show the statistical and systematic uncertainties added in quadrature.

The FONLL calculations [3], that are developed to obtain reliable predictions in the conditions $p_{T,Q} \sim m_Q$, provide the most stable description of data. For this reason it has been chosen to show a comparison between the CMS data and the previous measurements obtained within the LHC collaborations, with the aim to study the evolution of the cross section as a function of the center of mass energy and with respect to the different kinematic regions analyzed. Here a small selection is presented, only for the D^* meson, to show the results of this comparison in two different scenarios: same acceptance but lower center of mass energy, and complementary acceptance but same center of mass energy. For the first case the ATLAS [4] results are shown in Figure 2 (left) together with the CMS ones, with the data points compared to the respective FONLL predictions. Since the same

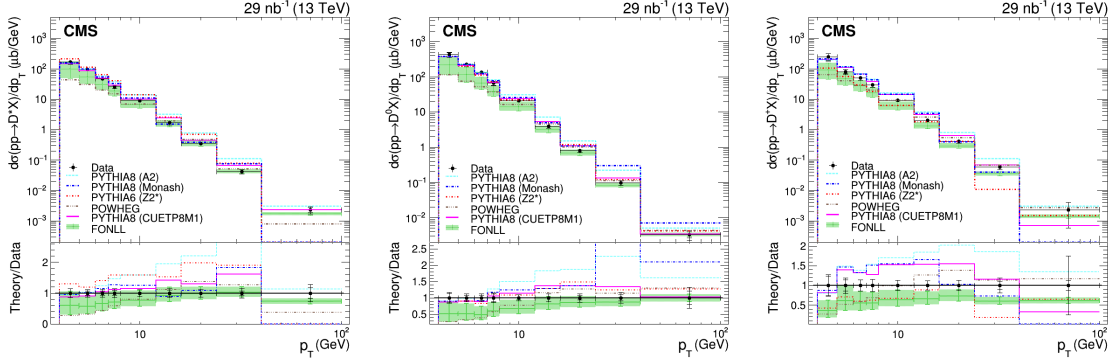


Figure 1: Differential cross section $d\sigma/dp_T$ for the D^{*+} , D^0 , and D^+ mesons. Black markers represent the data and are compared with several MC simulation models and theoretical predictions. The statistical and total uncertainties are separated by horizontal marks. On the lower panel of the figures, the ratio of the predictions to the central value of the data is shown [1].

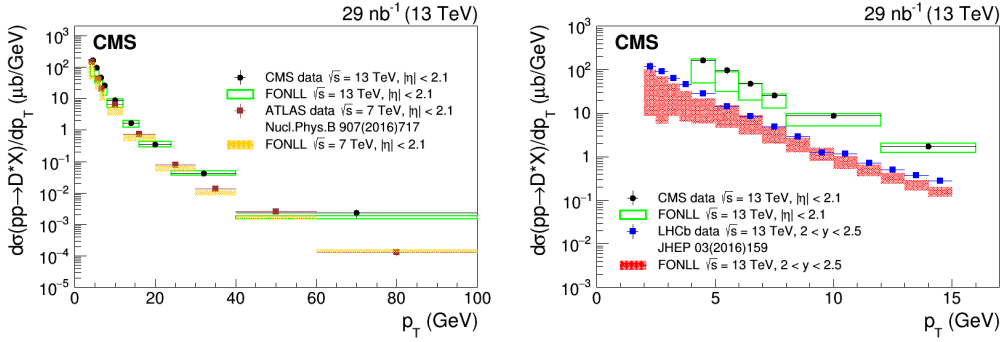


Figure 2: On the left: differential cross section $d\sigma/dp_T$ for the D^{*+} meson production, comparing the CMS (circles) and ATLAS (squares) data points to the respective FONLL predictions at $\sqrt{s} = 13$ TeV (empty boxes) and 7 TeV (filled boxes). On the right: differential cross section $d\sigma/dp_T$ for the D^{*+} meson production, comparing the CMS measurements at $\sqrt{s} = 13$ TeV (circles) and the LHCb points (squares) in the region $2 < y < 2.5$ at 13 TeV to the respective FONLL predictions (empty and filled boxes) [1].

acceptances are used, the scaling with the center of mass energy, from 7 to 13 TeV, can be directly observed. The other case is represented by LHCb, which performed the measurement at $\sqrt{s} = 13$ TeV but in a complementary acceptance region [5]. Figure 2 (right) shows only the closest rapidity bin analysed by LHCb ($2 < y < 2.5$) compared to the CMS data, to avoid a too much crowded comparison. Furthermore, the CMS data are reported only up to 16 GeV, following the LHCb endpoint, to make a more direct parallel between the two measurements. For both the comparisons, the measurements follow the FONLL predictions, thus the scaling does as well.

2. Relative cross sections of the $B_c^+(2S)$ and $B_c^{*+}(2S)$ states with respect to the B_c^+ state

Since the first observation of the $B_c^+(2S)$ and $B_c^{*+}(2S)$ [6], the $B_c^+(2S)$ to B_c^+ and $B_c^{*+}(2S)$ to B_c^+ , and the $B_c^{*+}(2S)$ to $B_c^+(2S)$ cross section ratio, are measured in proton-proton collisions at $\sqrt{s} = 13$ TeV, using a data sample collected by the CMS experiment, corresponding to an integrated luminosity of 143 fb^{-1} [7]. The three measurements are provided in the B_c^+ phase space window, with the excited $B_c^{(*)+}(2S)$ states reconstructed in their $B_c^+\pi^+\pi^-$ decay. The high-level trigger requires an opposite-sign muon pair of invariant mass 2.9-3.3 GeV, a dimuon vertex fit χ^2 probability larger than 10%, a distance of closest approach between the two muons smaller than 0.5 cm, and a distance between the dimuon vertex and the beam axis larger than three times its uncertainty. Both muons must have $p_T > 4$ GeV and $|\eta| < 2.5$ and the dimuon p_T must be aligned with the transverse displacement vector. In addition, a third track in the event is required, compatible with being produced at the dimuon vertex. The offline reconstruction requires two oppositely charged muons matching the triggered ones, tightening some cuts as described in [7].

The $B_c^+ \rightarrow J/\psi\pi^+$ candidates are reconstructed through a kinematic vertex fit, combining the dimuon with a track, imposing a common vertex. The B_c^+ candidates are required to have $p_T > 15$ GeV, $|\eta| < 2.4$, a kinematic vertex fit χ^2 probability larger than 10%, and a decay length (distance between the $J/\psi\pi^+$ vertex and the PV) larger than $100 \mu\text{m}$. If several B_c^+ candidates are found in the same event, only the one with the highest p_T is kept. An unbinned maximum-likelihood fit is applied to the $J/\psi\pi^+$ candidates invariant mass distribution. The B_c^+ peak is modelled by the sum of two Gaussian functions with a single mean and different widths. The underlying background is modelled as the sum of three terms: a first-order polynomial for the uncorrelated J/ψ -track combinations, an ARGUS function for the partially reconstructed $B_c^+ \rightarrow J/\psi\pi^+X$ decays, and a small contribution from $B_c^+ \rightarrow J/\psi K^+$ decays, with a shape fixed from simulation studies.

The $B_c^+(2S)$ and $B_c^{*+}(2S)$ candidates are also reconstructed through vertex kinematic fits, combining a B_c^+ candidate with two opposite-sign tracks, assumed to be the pions. Since the lifetimes of the $B_c^+(2S)$ and $B_c^{*+}(2S)$ are assumed to be negligible with respect to the measurement resolution, the production and decay vertices essentially coincide. The $B_c^+\pi^+\pi^-$ candidates must have $|\eta| < 2.4$ and a vertex kinematic fit χ^2 probability larger than 10%. Again, in case multiple candidates are found in the same event, only the one with the highest p_T is kept. For this decay the $M(B_c^+\pi^+\pi^-) - M(B_c^+) + m_{B_c^+}$ distribution, where $M(B_c^+\pi^+\pi^-)$ and $M(B_c^+)$ are the reconstructed invariant mass of the $B_c^+\pi^+\pi^-$ and B_c^+ candidates respectively, and $m_{B_c^+}$ is the world-average B_c^+ mass [2], is used to extract the number of events, since it has better resolution than $M(B_c^+\pi^+\pi^-)$. The measured distribution is fitted to a superposition of two Gaussian functions, each of them representing one of the two signal peaks, plus a third order Chebyshev polynomial, modelling the continuum background. Two background contributions arising from $B_c^+ \rightarrow J/\psi K^+$ decays are also considered, one for each peak, with shapes identical to those of the signal peaks. The two resonances are well resolved, with a mass difference of $\Delta M = 29.1 \pm 1.5$ MeV.

Several systematic uncertainties have been studied in the analysis, with the most important ones that come from the fit modelling and the dipion tracking efficiency.

The $B_c^{(*)+}(2S)$ to B_c^+ and the $B_c^{*+}(2S)$ to $B_c^+(2S)$ cross section ratios are derived from the

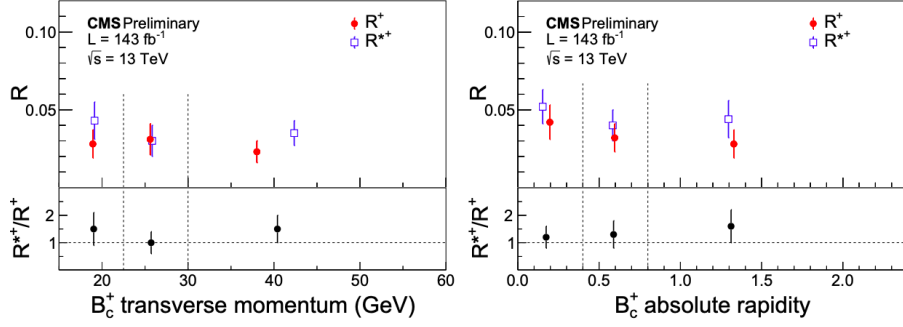


Figure 3: The R^+ , R^{*+} , and R^{*+}/R^+ cross section ratios as a function of the B_c^+ p_T (left) and the B_c^+ $|y|$ (right) [7].

measured yield ratios, correcting them for the detection efficiencies, ϵ :

$$\begin{aligned}
 R^+ &\equiv \frac{\sigma(B_c^+(2S))}{\sigma(B_c^+)} \mathcal{B}(B_c^+(2S) \rightarrow B_c^+ \pi^+ \pi^-) = \frac{N(B_c^+(2S))}{N(B_c^+)} \frac{\epsilon(B_c^+)}{\epsilon(B_c^+(2S))} = 3.57 \pm 0.69(\text{stat}) \pm 0.32(\text{syst})\%, \\
 R^{*+} &\equiv \frac{\sigma(B_c^{*+}(2S))}{\sigma(B_c^+)} \mathcal{B}(B_c^{*+}(2S) \rightarrow B_c^+ \pi^+ \pi^-) = \frac{N(B_c^{*+}(2S))}{N(B_c^+)} \frac{\epsilon(B_c^+)}{\epsilon(B_c^{*+}(2S))} = 4.91 \pm 0.69(\text{stat}) \pm 0.57(\text{syst})\%, \\
 R^{*+}/R^+ &= \frac{\sigma(B_c^{*+}(2S))}{\sigma(B_c^+(2S))} \frac{\mathcal{B}(B_c^{*+}(2S) \rightarrow B_c^+ \pi^+ \pi^-)}{\mathcal{B}(B_c^+(2S) \rightarrow B_c^+ \pi^+ \pi^-)} = \frac{N(B_c^{*+}(2S))}{N(B_c^+(2S))} \frac{\epsilon(B_c^+(2S))}{\epsilon(B_c^{*+}(2S))} = 1.39 \pm 0.35(\text{stat}) \pm 0.09(\text{syst})
 \end{aligned} \tag{2}$$

where the \mathcal{B} factors represent the branching fractions of the two $B_c^+ \pi^+ \pi^-$ decay channels. In order to probe if these cross section ratios show a dependence on the kinematics of the B_c^+ meson, the analysis has been repeated after splitting the events in three B_c^+ p_T bins and (independently) in three B_c^+ $|y|$ bins, as reported in figure 3. None of the measured ratios shows significant variations with the p_T or $|y|$ of the B_c^+ meson, the trends are perfectly compatible with flat functions within the probed kinematic regions.

3. Conclusion

In this paper the latest results about the D and B mesons production have been presented. The first measurement of the open-charm production cross section in pp collision in the Compact Muon Solenoid (CMS) experiment, using 2016 data, has been described. CMS measurements show a good agreement with the previous ones performed at the Large Hadron Collider (LHC), considering the evolution in the center of mass energy scale and the kinematic dependences, as described by the theory predictions. The latest results about the B_c mesons have been also presented: the $B_c^+(2S)$ to B_c^+ and $B_c^{*+}(2S)$ to B_c^+ , and the $B_c^{*+}(2S)$ to $B_c^+(2S)$ cross section ratios. No significant dependences on the p_T or $|y|$ of the B_c^+ mesons have been observed. The results of these measurements provide important input for the improvement of the theoretical understanding of the heavy flavour states and their production.

References

- [1] "Measurement of prompt open-charm production cross sections in proton-proton collisions at $\sqrt{s} = 13$ TeV", CMS Collaboration, CMS-PAS-BPH-18-003, <http://cds.cern.ch/record/2720606>
- [2] "Review of particle physics", Particle Data Group Collaboration, Phys. Rev. D 98 (2018) 030001, doi:10.1103/PhysRevD.98.030001
- [3] "The p_T spectrum in heavy flavor hadroproduction", M. Cacciari, M. Greco, and P. Nason, JHEP 05 (1998) 007, doi:10.1088/1126-6708/1998/05/007, arXiv:hep-ph/9803400
- [4] "Measurement of $D^{*\pm}$, D^\pm and D_s^\pm meson production cross sections in pp collisions at $\sqrt{s} = 7$ TeV with the ATLAS detector", ATLAS Collaboration, Nucl. Phys. B 907 (2016) 717, doi:10.1016/j.nuclphysb.2016.04.032.
- [5] "Measurements of prompt charm production cross-sections in pp collisions at $\sqrt{s} = 13$ TeV", LHCb Collaboration, JHEP 03 (2016) 159, doi:10.1007/JHEP03(2016)159, arXiv:1510.01707. [Erratum: JHEP 09, 013 (2016), Erratum: JHEP 05, 074 (2017)].
- [6] "Observation of two excited B_c^+ states and measurement of the $B_c^+(2S)$ mass in pp collisions at $\sqrt{s} = 13$ TeV ", CMS Collaboration, Phys. Rev. Lett. 122, 132001
- [7] "Relative cross sections of the $B_c^+(2S)$ and $B_c^{*+}(2S)$ and states with respect to the B_c^+ state in proton-proton collisions at $\sqrt{s} = 13$ TeV", CMS Collaboration, CMS-PAS-BPH-19-00, <http://cds.cern.ch/record/2718820>